TISSUE ENGINEERING: Part A
Volume 15, Number 11, 2009

DOI: 10.1089/ten.tea.2009.0064

Original Article

The Human Umbilical Vein with Wharton's Jelly as an Allogeneic, Acellular Construct for Vocal Fold Restoration

Roger W. Chan,[1] Maritza L. Rodriguez,[2] and Peter S. McFetridge[2]

This study investigated the potential of the decellularized human umbilical vein (HUV) as an allogeneic, acellular extracellular matrix (ECM) scaffold for engineering the vocal fold lamina propria *in vitro*. HUV specimens with Wharton's jelly on the abluminal surface were uniformly dissected from native umbilical cords using an automated procedure and subjected to a novel saline-based decellularization treatment for removal of potentially antigenic epitopes. Human vocal fold fibroblasts from primary culture were seeded onto the resulting acellular constructs and cultured for 21 days. The structures of decellularized and fibroblast-repopulated HUV constructs and the attachment, proliferation, and infiltration of fibroblasts were examined with light microscopy and scanning electron microscopy. Changes in the relative densities of collagen in the constructs associated with decellularization and recellularization were quantified using digital image analysis. In addition, fibroblasts infiltrating the scaffolds were released by cell recovery and quantified by counting. Viscoelastic properties of the scaffolds were measured using a linear, simple-shear rheometer at phonatory frequencies. Results showed that an acellular ECM construct with an intact three-dimensional structure of Wharton's jelly was fabricated. Vocal fold fibroblasts readily attached on the abluminal surface of the construct with high viability, with significant cellular infiltration up to approximately 600 μm deep into the construct. A significant increase in collagen expression was observed with recellularization. The elastic modulus and dynamic viscosity of the fibroblast-repopulated scaffolds were comparable to those of the human vocal fold lamina propria. These findings supported the potential of the construct as a possible surgical allograft for vocal fold restoration and reconstruction.

Introduction

Despite significant advances in laryngeal surgery in the past decade, laryngeal pathologies involving the connective tissue layer or lamina propria of the human vocal fold constitute one of the most significant challenges for clinicians and surgeons.[1–3] For debilitating vocal fold disorders and injuries requiring the removal and replacement of lesions and deficiencies in the lamina propria, such as scarring, sulcus vocalis, and atrophy, it is essential to replace the defects with grafts or biomaterials that do not induce or aggravate fibrosis and scar tissue formation.[2] It is also important for these implants to have viscoelastic properties similar to those of the native vocal fold lamina propria, such that they are conducive to vocal fold vibration and phonation (voice production) through the transfer of aerodynamic energy into acoustical energy.[4,5]

Some recent studies on the use of hyaluronic acid (HA)-based and collagen-based hydrogels have demonstrated their potential as tissue replacement for such pathologies, in order that constructive extracellular matrix (ECM) remodeling of the lamina propria and favorable viscoelastic properties of the resulting tissue constructs may be facilitated.[6–9] An equally promising alternative is the use of acellular biological ECM scaffolds, derived from decellularization of native connective tissues. Acellular ECM scaffolds have shown considerable promise for tissue regeneration in various tissue systems in the body, including heart valves, blood vessels, peripheral nerves, urinary bladder, and musculoskeletal tissues.[10–15] In previous studies, we have developed an acellular scaffold derived from the bovine vocal fold lamina propria as a potential xenograft for the human vocal fold.[16,17] A novel saline-based osmotic approach for decellularization of the native bovine vocal fold was developed to fabricate acellular scaffolds. This decellularization approach was being used in the current study to fabricate an allogeneic, acellular construct from the human umbilical cord, specifically

[1]Otolaryngology – Head and Neck Surgery, Biomedical Engineering, University of Texas Southwestern Medical Center, Dallas, Texas.
[2]Mammalian Cell and Organ Culture Laboratory, School of Chemical, Biological and Materials Engineering, University of Oklahoma, Norman, Oklahoma.

the human umbilical vein (HUV) with Wharton's jelly on its abluminal surface.

The human umbilical cord consists of two arteries, one vein, and Wharton's jelly, the connective tissue layer that is primarily an ECM in the cord.[18] The major advantage of the use of the umbilical cord as a potential vocal fold scaffold is that a properly dissected umbilical vein or artery presents a layer of Wharton's jelly on its abluminal surface. Wharton's jelly is an ECM rich in a variety of fibrous proteins, interstitial proteins, and signaling molecules, including glycosaminoglycans (GAGs), proteoglycans, and peptide growth factors, all of which could facilitate cellular attachment, proliferation, infiltration, and differentiation, leading to constructive ECM remodeling and tissue reconstruction. In general, acellular scaffolds are composed of key matrix proteins and signaling molecules that are optimally distributed spatially for constructive tissue remodeling.[10,19] Wharton's jelly in the human umbilical cord was targeted in the current study because it is composed of a variety of peptide growth factors, including insulin-like growth factor I (IGF-I), fibroblast growth factor (FGF), transforming growth factor beta 1 (TGF-β1), platelet-derived growth factor (PDGF) and epidermal growth factor (EGF).[20] These growth factors contribute to regulate the cellular proliferation, differentiation, synthesis, and degradation of many of the critical matrix proteins in the vocal fold ECM, including collagen, elastin, GAGs, and proteoglycans.[16,21,22]

Daniel *et al.* developed an automated procedure for dissection of the human umbilical cord, capable of producing highly repeatable HUV specimens with precisely defined geometry.[23] The procedure involved freezing native umbilical cord specimens on a stainless steel mandrel, with the dissection performed using a high-speed steel cutting tool with the tissue and mandrel secured on a modified lathe. It was found that the dissected umbilical vein or artery specimens were highly uniform, with a thickness of approximately 750 μm. Mechanical testing revealed that they had appropriate compliance, burst pressure, suture holding capacity, and biphasic stress–strain relationships for potential use as small blood vessel grafts.[23]

Using a novel saline-induced osmotic treatment approach,[16] the HUV with Wharton's jelly was decellularized to fabricate an acellular scaffold in the current study. The acellular scaffold was then repopulated with human vocal fold fibroblasts from primary culture. Structures of the decellularized and recellularized constructs were examined histologically. Repopulation of the acellular scaffolds with vocal fold fibroblasts, including their attachment and infiltration, was examined with light microscopy and scanning electron microscopy (SEM). The expressions of collagen in the constructs were estimated using digital image analysis of tissue sections stained with Masson's trichrome. Fibroblasts infiltrating the scaffolds were released and quantified by cell recovery and counting to assess their rate of proliferation. Viscoelastic shear properties of the acellular and fibroblast-repopulated scaffolds relevant to phonation were measured using a simple-shear rheometer in the physiological frequency range,[24] to estimate their biomechanical, performance in the context of functional vocal fold restoration.

Materials and Methods

Human umbilical cord tissues

Thirteen human umbilical cord specimens were harvested from healthy newborns at a local hospital in Norman, Oklahoma; stored in isotonic phosphate buffered saline (PBS) solution with the antibiotics penicillin (100 U/mL) and streptomycin (1 mg/mL) (Sigma, St. Louis, MO) at 4°C overnight; and frozen at −80°C onto 6-mm steel mandrels for 2 days in preparation for an automated dissection procedure. The institutional review board of the University of Oklahoma approved the tissue procurement and experimental protocols. Following Daniel *et al.*,[23] the automated dissection procedure involved the use of a high-speed steel cutting tool with the tissue-on-mandrel complex secured on a modified lathe, resulting in a uniform tissue thickness of 750 μm when frozen and approximately twice of that (~1500–1650 μm) after thawing because of thermal expansion and hydration. In the frozen tissue, the endothelium was found on the luminal surface of the tubular-shaped umbilical vein specimen, followed by the smooth muscle layer of the vein with a depth of 200 to 400 μm. Wharton's jelly made up the remaining thickness of the specimen. After dissection, each HUV specimen remained frozen at −20°C for 4 days and was thawed by immersion in double distilled water at 5°C for 1 h. A 5.0-mm-long section on each end of each dissected HUV specimen was discarded to eliminate irregularities in boundary geometry.

Table 1. Experimental Design Indicating the Number of Sections for the Characterization of the Human Umbilical Vein (HUV) Specimens, the Decellularized Constructs, and Their Repopulation by Vocal Fold Fibroblasts at Different Time Points

			Fibroblast-repopulated scaffolds								
			Days in culture								
Experimental characterization	*Native umbilical cord specimens*	*Acellular HUV constructs*	0	1	3	6	9	12	15	18	21
SEM		3									3
Light microscopy with H&E and Alcian blue	3	3									3
Light microscopy with trichrome (for image analysis)	3	3									3
Cell recovery (cell proliferation)			3	3	3	3	3	3	3	3	3
Rheometric testing	6	3									3

The HUV specimen was then cut longitudinally, opened, and sliced into five rectangular tissue sections with dimensions of approximately 10.0 mm×17.0 mm each.

Table 1 shows the details of the experimental design involving different treatment of the specimen sections, the number of sections, and the experimental methods used to characterize them. A total of 65 sections were obtained from the 13 HUV specimens. Twelve of the 65 sections (from 6 cords) were not subjected to further treatment, because these native HUV sections were subjected to histological examination using hematoxylin and eosin (H&E) staining, staining with Masson's trichrome, and rheometric measurements with a linear, simple-shear rheometer (details in the following sections). Fifty-one of the other 53 sections (from 13 cords) were mounted on plastic support frames at a uniform tension for subsequent decellularization. Twelve of these 51 decellularized sections were not subjected to further treatment, because these acellular HUV sections were assessed by: (1) ultrastructural examination with SEM, (2) H&E staining, (3) trichrome staining, and (4) rheometric measurements of tissue viscoelastic properties. The other 39 decellularized sections were recellularized and cultured for up to 21 days, with 27 recellularized sections assigned for cell recovery experiments (for measurement of cell proliferation) and 12 recellularized sections assigned for the same methods of experimental assessment as for the 12 acellular sections, as shown in Table 1.

Decellularization protocol

Fifty-one of the 65 auto-dissected HUV sections harvested from 13 umbilical cords were mounted on plastic support frames, washed in PBS solution with antibiotics, and decellularized. The decellularization procedure was based on the novel osmotic approach of Xu *et al.*,[16] with the durations of the various steps adjusted to maximize the extent of decellularization while minimizing structural damage to the three-dimensional (3-D) protein network, according to results of preliminary studies.[25] The first step of the decellularization involved soaking the sections in 3M sodium chloride solution at 25°C for 12 h, inducing osmotic stress on native endothelial cells, fibroblasts, myofibroblasts, and macrophages. Next, the sections were incubated in PBS solution with RNAse (10 μg/mL) and DNAse (25 μg/mL) (Sigma) at 37°C for 12 h to lyse the cells and degrade any exposed nucleic acids. The third step was to dehydrate the sections in 75% ethanol at room temperature for 6 h to initiate a new cycle of osmotic stress. Finally, the sections were again incubated in PBS solution containing 10 μg/mL RNAse and 25 μg/mL DNAse at 37°C for another 12 h. Once these steps were completed, the sections were washed in PBS solution with antibiotics (100 U/mL penicillin and 1.0 mg/mL streptomycin) at room temperature to remove any remaining cellular debris along with previously added reagents. The decellularized scaffolds were stored in this solution at 4°C for up to 3 days, ready for further experimentation. Just before cell seeding, scaffolds were sterilized again in 70% ethanol under ultraviolet light.

Human vocal fold fibroblasts

A hemilarynx was procured from a 60-year-old Hispanic man who underwent total laryngectomy because of supraglottic cancer not involving the true vocal folds. The subject was a non-smoker. A laryngologist and a pathologist examined his vocal folds and judged them to be free of any benign or malignant lesions. The Institutional Review Board of the University of Texas Southwestern Medical Center approved the tissue procurement and experimental protocols. Primary cell culture of vocal fold fibroblasts was obtained based on the primary explant technique, as detailed before.[16] Serial passaging of the vocal fold fibroblasts was performed with trypsinization (0.25% trypsin and 0.02% ethylenediaminetetraacetic acid (EDTA)). Fibroblasts of an early passage (passage 4) were used for the current study, with the primary cells at a growth stage before the onset of replicative senescence or *in vitro* aging in culture.[26]

Fifty-one acellular HUV scaffold sections, each with dimensions of approximately 10 mm by 17 mm by 1650 μm, were obtained from the decellularization as described above. Thirty-nine of these acellular HUV scaffolds were seeded with the primary-culture human vocal fold fibroblasts at a density of 1 million cells per scaffold (10^6 cells resuspended in 100 μL of Dulbecco's modified Eagle medium with 10% fetal bovine serum).

Tissue culture

Of the 39 recellularized scaffolds, 12 (from 4 cords) were cultured for 21 days at 37°C, with medium changes every other day. After 21 days of culture, the scaffolds were removed from the plastic mounting frames and examined by the same experimental assessment as for the 12 acellular sections that were not recellularized: (1) SEM, (2) light microscopy with H&E staining, (3) trichrome staining, and (4) rheometric measurements of viscoelastic shear properties (Table 1). The other 27 recellularized scaffolds (from 9 cords) were cultured in groups of three for nine different time periods, ranging from 1 h (0 days) to 21 days (Table 1). Afterwards, they were subjected to cell recovery experiments for the assessment of proliferation of the cells as a function of time in culture.

Cell recovery

The procedure for the recovery of fibroblasts infiltrating the HUV constructs and the subsequent counting of the cells released was based on the method of Xu *et al.*[16] Briefly, each scaffold was incubated in 0.25% trypsin and EDTA solution (Sigma) at 37°C for 45 min, with mechanical agitation every 15 min to release the cells from the scaffold. The total number of cells released from the scaffold was measured using a hemocytometer under a light microscope. Twenty-seven recellularized scaffolds at nine time points (1 h (0 days) and 1, 3, 6, 9, 12, 15, 18, and 21 days after cell seeding) were subjected to cell recovery, with three scaffolds trypsinized at each time point.

Scanning electron microscopy

The abluminal surface of the acellular HUV scaffolds and the fibroblast-repopulated scaffolds were observed with SEM to evaluate the 3-D morphological structure of the constructs and the attachment of fibroblasts. First, specimens for SEM examination were fixed in 2.5% glutaraldehyde solution with 0.1M cacodylate buffer. Next, the samples were washed in the cacodylate buffer solution three times, each for 5 min, followed by postfixation in buffered 1% osmium tetroxide

solution for 1 h. Samples were then washed with the buffer again three times, dehydrated with graded ethanol treatment (50%, 70%, 95%, and 100% v/v for 10–30 min each), and subjected to critical-point drying, mounting, and gold-sputtering. A JEOL JSM-840A scanning electron microscope (JEOL Inc., Peabody, MA) was used for the examination and image acquisition. SEM images were taken at magnifications of 500× and 1000×.

Histological examination with H&E staining, Alcian blue, and Masson's trichrome

Native HUV sections, acellular HUV scaffolds, and fibroblast-repopulated scaffolds were examined histologically. Specimens were fixed in 10% neutral buffered formalin, dehydrated with graded ethanol treatment, and embedded in paraffin. They were cut into sections of 5.0 μm using a microtome and mounted on glass slides. H&E staining was performed to examine the histological structure of the specimens and the cellular attachment, proliferation, and infiltration, whereas the level of GAGs in the acellular construct was examined with Alcian blue staining. The slides were deparaffinized in xylene, rehydrated, and stained with H&E and Alcian blue following standard protocol.[27] Masson's trichrome was used to estimate the overall level of collagen in the specimens, with an intense staining color of blue. The slides were deparaffinized in xylene, rehydrated, and stained with Bouin's solution, Weigert's iron hematoxylin solution, Biebrich scarlet-fuchsin solution, and aniline blue solution for trichrome staining according to standard protocol.[27]

Digital image analysis

The relative densities of collagen in the histological sections stained by Masson's trichrome were estimated from the staining intensities and relative areas of collagen using digital image analysis with Image J (National Institutes of Health, Bethesda, MD). Masson's trichrome did not differentiate different types of collagen; hence, the staining intensities reflected the total of all collagen types stained. The image analysis process was based on that of Chan *et al.*[28] and Xu *et al.*[29] Briefly, color images were first converted to 8-bit grayscale images, with the grayscale values for each image unit (or pixel) ranging from 0 (black) to 255 (white) (minimum intensity to maximum intensity). A threshold intensity value was selected for each image within this range of grayscale values such that the pixels representing the areas of collagen in the image matched with those in the corresponding color image. Pixels with intensity values lower than the threshold value (between 0 and the threshold) were deemed representative of collagen in the image. The relative density of collagen was then calculated as the fraction of the positively stained area to the total area of the section. The reliability of this image analysis procedure was examined in our previous study,[29] showing that the intrarater and interrater reliability were high, with mean percentage differences in the measurements smaller than 4% in all cases.

Rheometric measurement of viscoelastic properties

A novel controlled-strain, linear simple-shear rheometer, as reported in Chan and Rodriguez, was employed to quantify the biomechanical properties of the various specimens.[24] This system applies a translational, linear oscillatory shear deformation to determine the viscoelastic shear properties of tissue samples, including the elastic shear modulus (G') and the dynamic viscosity (η'). The system has been validated by identifying the frequency responses of key system components, with results indicating that valid rheometric measurements could be made in the phonatory frequency range, up to 250 Hz.[24] The principle of the simple-shear rheometry is shown in Figure 1, where a tissue sample of area A is sandwiched between two rigid parallel plates with a gap size d, with a linear motor delivering a translational shear of a specified amplitude (x) and frequency to the sample through the upper plate. Through the lower plate, a piezoelectric force transducer detects the shear force (F) resulting from the viscoelastic response of the sample. All empirical measurements of tissue viscoelastic shear properties were conducted in an environmental chamber, which maintained a temperature of 37°C and close to 100% relative humidity to prevent tissue dehydration.

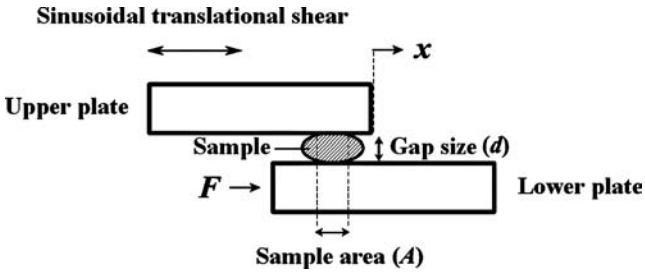

FIG. 1. The principle of simple-shear rheometry for the measurements of viscoelastic shear properties. Shear stress is given by the ratio of the shear force F to the sample area A, whereas shear strain is defined as the ratio of the displacement x to the gap size d. According to the theory of linear viscoelasticity, the elastic shear modulus (G') and dynamic viscosity (η') of the sample can then be quantified as a function of frequency, up to 250 Hz.

Statistical analysis

For the cell recovery results, the nonparametric Kruskal-Wallis test was conducted to determine whether the number of cells released from the recellularized HUV scaffolds increased significantly over time. For the results of the quantitative digital image analysis, the Friedman test was used to determine whether the relative staining intensities of collagen in the native HUV specimens, the decellularized HUV constructs, and the fibroblast-repopulated scaffolds were significantly different from one another. Nonparametric statistical tests were used because of a lack of evidence on the validity of the assumptions of normality of distributions and homogeneity of variances required for parametric tests. The level of significance (alpha) was set at 0.05.

Results and Discussion

Histology of native HUV specimens, acellular constructs, and recellularized scaffolds

Figure 2 shows the scanning electron micrographs of the abluminal surface of a decellularized HUV construct. It can be seen that the 3-D morphological structure of the ECM was

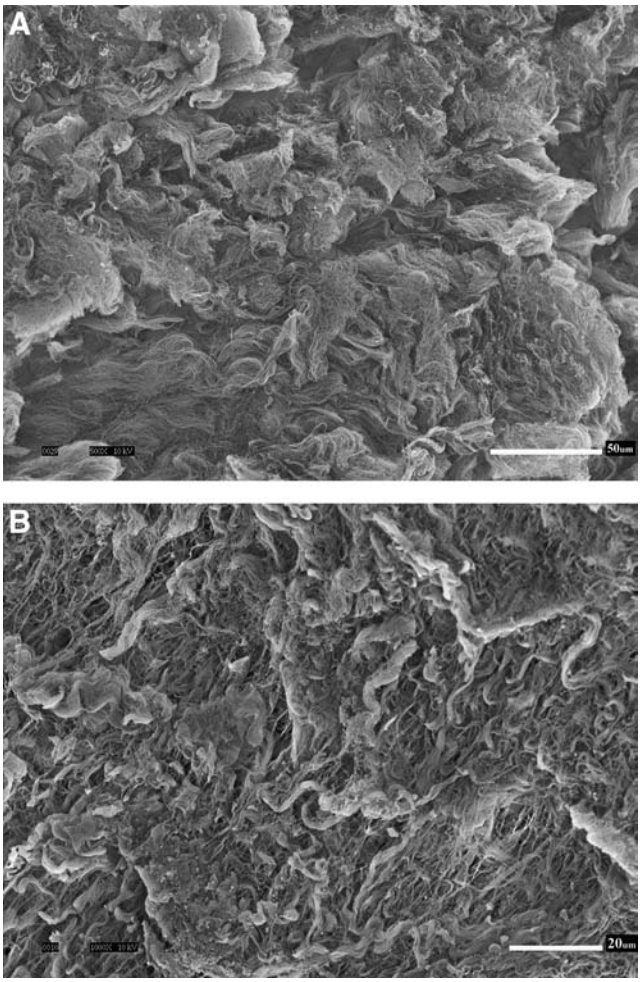

FIG. 2. Scanning electron micrographs showing the abluminal surface of the acellular human umbilical vein (HUV) construct, at a total magnification of (**A**) 500×, and (**B**) 1000×. Scale bars = 50 μm (for **A**), 20 μm (for **B**).

largely intact after the decellularization process, with the porous nature of Wharton's jelly visible at a higher magnification (Fig. 2B). No evidence of native cellular structures from the umbilical vein can be observed in the SEM micrographs. Figure 3 shows the histological sections of the native HUV specimens (Fig. 3A, B), the acellular HUV scaffolds (Fig. 3C–F), and the fibroblast-repopulated scaffolds (Fig. 3G, H). All sections were stained with H&E, except for Figure 3F, which was stained with Alcian blue at pH 2.5. For each photomicrograph, the abluminal surface (Wharton's jelly) faces toward the left, and the luminal surface (endothelium) is on the right. Based on these figures, it was evident that decellularization had removed native cells found in the HUV specimens (Fig. 3A, B) throughout the entire acellular HUV construct (Fig. 3C–F). Alcian blue staining also demonstrated a widespread distribution of GAGs in the acellular construct (Fig. 3F). Significant attachment, proliferation, and infiltration of primary-culture human vocal fold fibroblasts can be observed in the recellularized scaffolds (Fig. 3G, H). Specifically, there were up to several layers of fibroblasts attaching to the abluminal surface of the scaffolds, and cellular infiltration could be seen up to a considerable depth of the construct (~600 μm), essentially the entire thickness of Wharton's jelly. This level of cellular infiltration was significantly higher than that observed previously for vascular scaffolds such as the porcine carotid artery,[14] and better than the infiltration shown for a bovine acellular scaffold fabricated in our laboratory using a similar saline-based decellularization approach.[16] SEM micrographs of the recellularized scaffolds show some primary-culture fibroblasts attaching to the abluminal surface (Fig. 4), where the cells were characterized by a lighter shade of gray, a 3-D appearance, an elongated morphology, and cytoplasmic processes. These morphological features suggested that the proliferating cells attached to the HUV scaffolds were viable.

Proliferation of vocal fold fibroblasts

The results of cell recovery are shown in Figure 5, illustrating the proliferation of primary-culture human vocal fold fibroblasts after being seeded in the decellularized HUV constructs. The number of cells released from the recellularized scaffold sections and recovered by trypsinization was quantified as a function of time in culture and normalized by the area of the scaffold sections. The data indicated a roughly exponential increase in cellular proliferation with time, with approximately 600 cells counted from each mm^2 of the scaffold 6 days after cell seeding, with the cumulative growth increasing to almost 10,000 cells per mm^2 in 21 days. Results of the nonparametric Kruskal-Wallis test confirmed that the number of cells increased significantly with time ($H = 9.97$, $p < 0.05$).

Image analysis of collagen expression

The relative densities of collagen expressed in the histological sections stained using Masson's trichrome were estimated from the staining intensities using a digital image analysis approach with Image J (National Institutes of Health). Results showed that the relative level of collagen decreased with the process of decellularization (Fig. 6), which may be related to some collagen fibrils being washed out from the constructs during the cycles of osmotic mechanical stresses. However, collagen density increased sharply upon recellularization, likely because of the synthesis of new collagen by the vocal fold fibroblasts in the recellularized HUV scaffolds. The Friedman test was conducted to examine whether the levels of collagen changed significantly with the processes of decellularization and recellularization. Results indicated that the relative densities of collagen expressed in the native HUV specimens, the decellularized HUV constructs, and the recellularized scaffolds were significantly different from one another (chi-square = 6, degrees of freedom = 2, $p < 0.05$).

Measurement of rheometric properties

The viscoelastic shear properties of the native HUV specimens, the acellular HUV constructs, and the fibroblast-repopulated scaffolds were quantified using a controlled-strain, linear simple-shear rheometer in the physiological frequency range of phonation (up to 250 Hz) to estimate their functional biomechanical performance. Figure 7 shows the elastic shear modulus (G') of the specimens as a function of frequency, in comparison with data of the human vocal fold lamina propria previously reported.[24] At phonatory

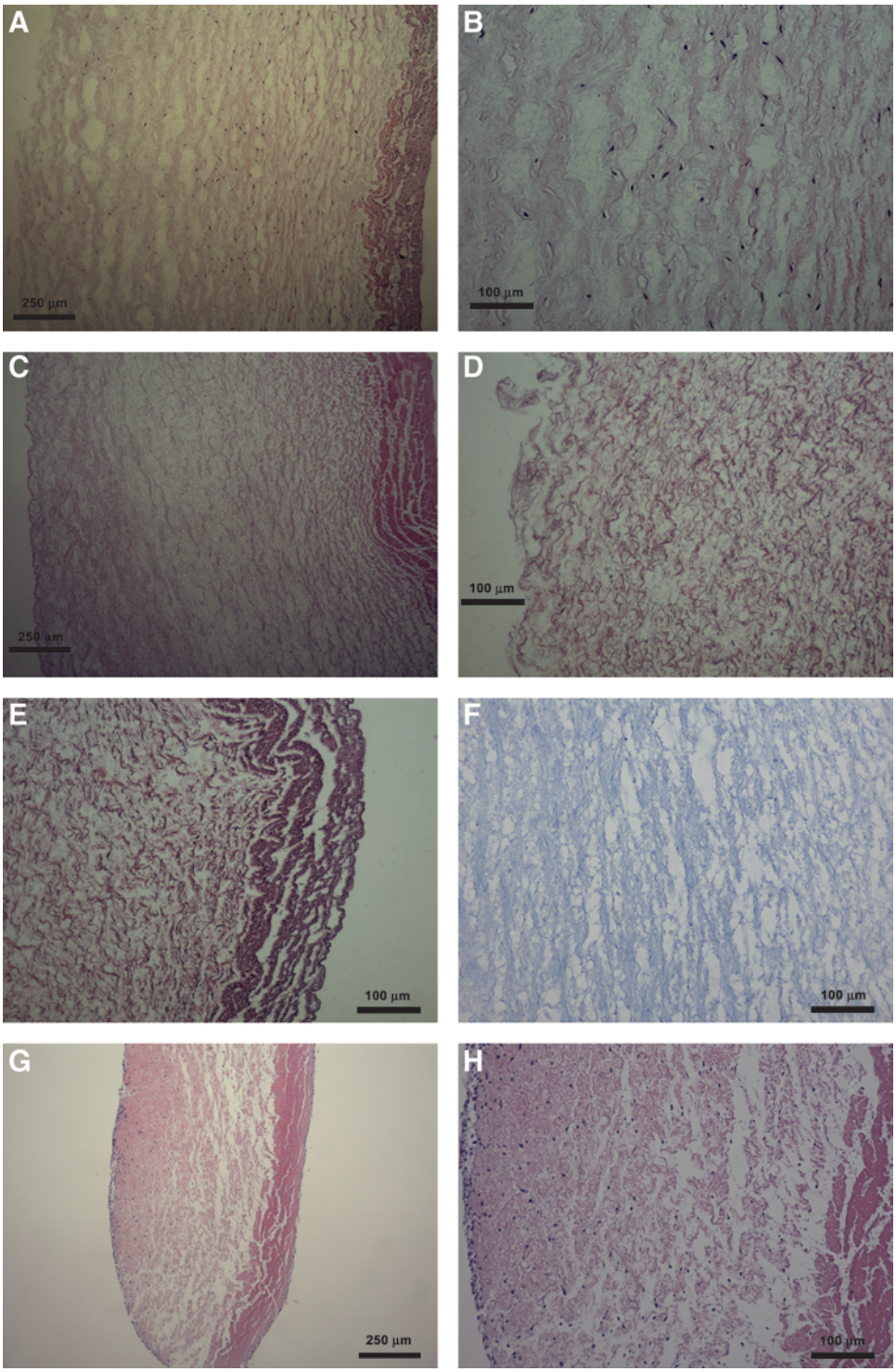

FIG. 3. Transverse sections of native HUV (**A**) at 40× and (**B**) at 100×; acellular HUV construct (**C**) at 40×, (**D**) at 100× (abluminal surface), (**E**) at 100× (luminal surface), and (**F**) at 100×; fibroblast-repopulated HUV scaffold 21 days after cell seeding (**G**) at 40×, and (**H**) at 100×. All sections were stained with H&E, except for (**F**), which was stained with Alcian blue at pH 2.5. In all figures, the luminal surface of the construct is oriented toward the right, and the abluminal surface is facing the left. Cross-sectional transition of the tissue layers from the lumen of the construct to the albumen can be clearly seen in (**A**), (**C**), and (**G**), from the endothelium to the smooth muscle layer to the extracellular Wharton's jelly (right to left). Native cellular structures observed in the auto-dissected HUV specimens (**A, B**) have been removed in the decellularized HUV construct (**C–F**), whereas significant attachment, proliferation, and infiltration of the primary human vocal fold fibroblasts can be readily seen in the recellularized scaffold (**G, H**).

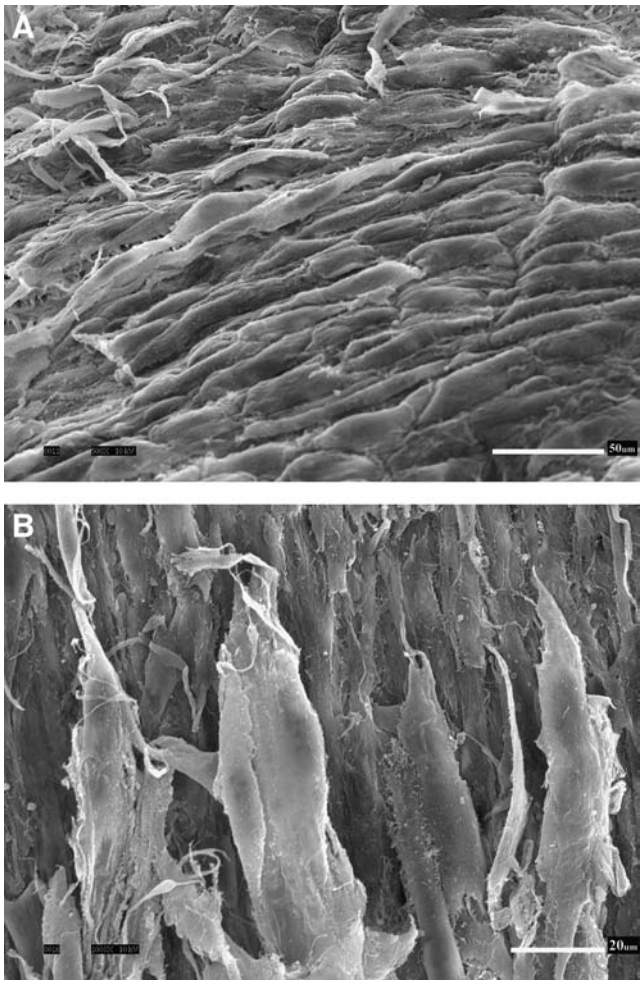

FIG. 4. Scanning electron micrographs showing the abluminal surface of the fibroblast-repopulated HUV scaffold, at (**A**) 500× and (**B**) 1000×. Scale bars = 50 μm (**A**), 20 μm (**B**).

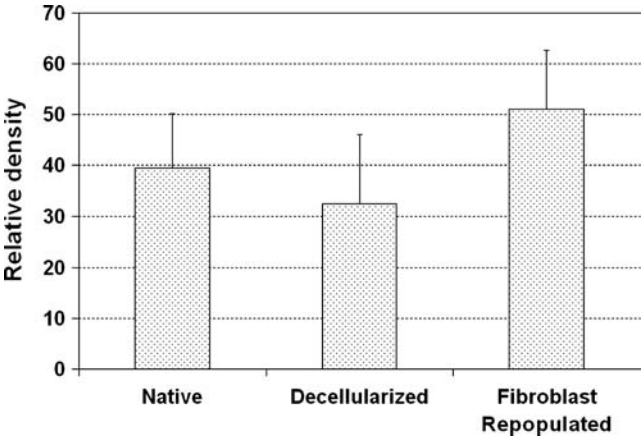

FIG. 6. Relative densities (staining intensities) of collagen fibers in native HUV specimens, acellular HUV constructs, and recellularized HUV scaffolds as estimated by digital image analysis of trichrome tissue sections (means + standard deviations; n = 3).

frequencies (>100 Hz), a higher G' was observed for the acellular HUV constructs than for the native HUV specimens, whereas a lower G' was evident for the recellularized scaffolds after being populated by primary-culture human vocal fold fibroblasts. The values of G' are indicative of tissue stiffness under shear deformation typically encountered during vocal fold vibration.[4] The acellular HUV constructs exhibited a tissue stiffness level close to that of the human vocal fold cover, whereas the native HUV specimens and the recellularized scaffolds showed a somewhat lower stiffness than that of the human vocal fold cover (Fig. 7).

The dynamic viscosity (η') for the different HUV specimens is a decreasing function of frequency (Fig. 8), demonstrating the phenomenon of shear-thinning, as shown previously with a bovine acellular scaffold and with human vocal fold tissues.[16,24] Similar to the trends observed for the elastic modulus, the acellular HUV constructs showed a higher dynamic viscosity than that of the native HUV specimens, and tissue

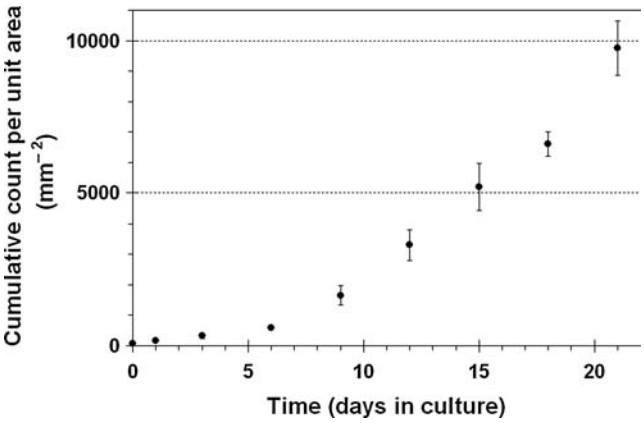

FIG. 5. Results of cell recovery showing the number of proliferating vocal fold fibroblasts released from the recellularized HUV scaffold as a function of time (cumulative data normalized by the scaffold unit area; means ± standard deviations; n = 3).

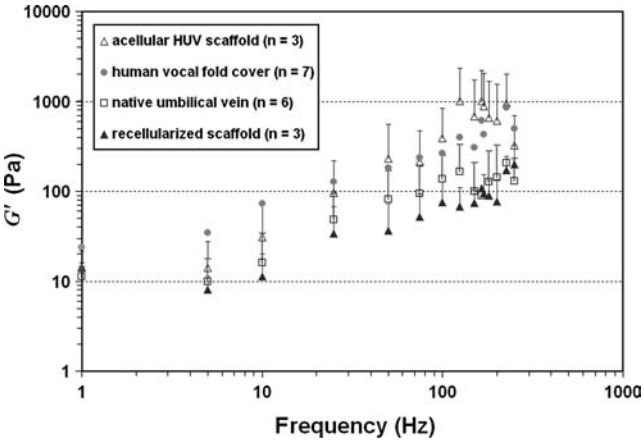

FIG. 7. Elastic shear modulus (G') of native human umbilical veins, acellular HUV constructs, and fibroblast-repopulated HUV scaffolds as a function of frequency (1–250 Hz). Data on the human vocal fold lamina propria (cover)[24] are also shown for comparison.

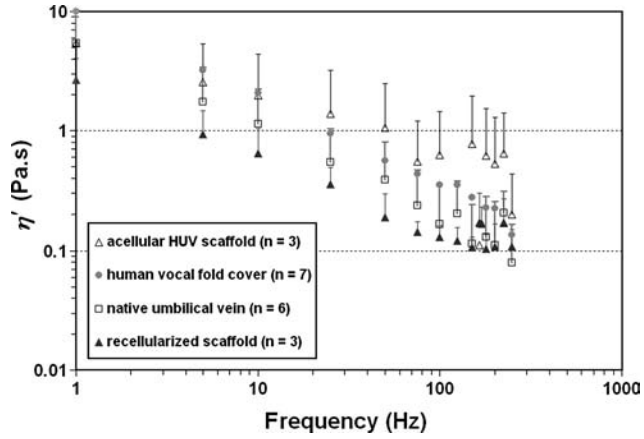

FIG. 8. Dynamic viscosity (η′) of native human umbilical veins, acellular HUV constructs, and fibroblast-repopulated HUV scaffolds as a function of frequency (1–250 Hz). Data on the human vocal fold lamina propria (cover)[24] are also shown for comparison.

viscosity decreased significantly upon recellularization with human vocal fold fibroblasts. The data values of η′ observed for the native HUV specimens and the recellularized scaffolds at phonatory frequencies were in the same range as those reported for the human vocal fold cover (Fig. 8).

These trends of differences in G' and η′ observed between the different HUV specimens (Fig. 7 and 8) could be attributed to the purported biomechanical effects of tissue structural changes associated with decellularization and recellularization. The observations of higher tissue stiffness and higher dynamic viscosity in the acellular HUV constructs may be related to the formation of a denser, more-compact network of matrix proteins upon decellularization (Fig. 3B, D), which has also been observed in the bovine acellular scaffold developed in our laboratory.[16] Furthermore, the increase in tissue viscosity could be linked to possible changes in tissue hydration following the cycles of osmotic stresses during decellularization. Hydration has been shown to play a key role in dictating the viscoelastic properties of vocal fold tissues,[30] and it was feasible that the cycles of osmotic stresses could lead to a lower level of tissue hydration, resulting in higher tissue viscosity (and perhaps stiffness). On the other hand, the significant decreases in tissue stiffness and viscosity observed upon recellularization were likely associated with the synthesis of new matrix proteins and their incorporation into the scaffold protein network. Lower G' and η′ were observed despite a higher collagen level in the recellularized scaffolds (Fig. 6). This finding was consistent with the reported absence of a significant correlation between collagen level and vocal fold tensile stiffness,[28] and could be related to the dominance of the effects of other matrix proteins over those of collagen in the construct, particularly GAGs (Fig. 3F). Overall, these patterns of changes in viscoelastic properties were quite similar to those reported previously for our bovine acellular scaffold.[16] Such viscoelastic properties being close to those of the human vocal fold lamina propria suggested that, functionally, the tissue construct should favor the initiation and sustaining of vocal fold vibration for phonation.[5]

General Discussion

The promise of the acellular tissue engineering construct developed in the current study was believed to be the layer of Wharton's jelly found on its abluminal surface, which is an ECM of a variety of proteins, including collagen (types I, II, III, IV, V, VI, and VII), laminin, peptide growth factors, GAGs, and proteoglycans.[20,31–34] The distribution of ECM proteins in Wharton's jelly has been examined using immunofluorescent imaging, demonstrating that collagen types I, II, and VI are homogeneously distributed throughout the entire layer of Wharton's jelly, enmeshed with fibrils of collagen type III and type IV, as well as laminin and heparan sulfate proteoglycans.[32] Collagen has been found to be the major matrix protein in Wharton's jelly, with the total content of collagen reported to be approximately 550 mg/g, or approximately 50% of the dry weight of defatted Wharton's jelly.[33] With differential salt precipitation techniques, four collagen types have been identified using sodium dodecyl sulfate polyacrylamide gel electrophoresis as types I, III, V, and VII, with type I being the most abundant (~50% of all types). The dominance of type I collagen in the acellular HUV construct, together with the rich collection of different collagen types, were quite similar to other acellular ECM scaffolds already in use, such as the porcine small intestinal submucosa and urinary bladder submucosa, which have been shown to degrade readily once implanted *in vivo* while promoting a constructive matrix remodeling response in the host.[10,11] The small intestinal submucosa and urinary bladder submucosa have been used as xenografts in a variety of tissue engineering applications, such as the reconstruction of musculoskeletal, cardiovascular, urinary, dural, and dermal tissues.

Of the GAGs in Wharton's jelly, HA was found to constitute approximately 70% of the total content of GAGs.[33] Because HA is multifunctional, being responsible for the maintenance of tissue hydration, tissue viscoelasticity, cellular proliferation, migration, cell surface receptor interactions, and collagen fibril size and density, amongst others,[35] its abundance in the acellular HUV construct is demonstrated with Alcian blue staining (Fig. 3F) and is consistent with the significant proliferation and infiltration of vocal fold fibroblasts observed (Figs. 3G, H), as well as the optimal viscoelastic properties of recellularized scaffolds shown in Figures 7 and 8. Significant amounts of sulfated GAGs have also been found in Wharton's jelly, forming predominantly chondroitin sulfate and dermatan sulfate proteoglycans, including decorin, biglycan, and versican.[31,34] These proteoglycans affect the matrix network organization of collagen fibrils and contribute to cell–cell and cell–ECM interactions. For example, decorin and biglycan co-regulate the diameter and organization of collagen fibrils, whereas versican can assist with the growth and proliferation of cells, destabilizing their adhesion to the ECM.[31,34] These proteoglycans also form a reservoir for binding a variety of growth factors, such as FGF, TGF-β1, PDGF, and EGF, to regulate cellular proliferation, differentiation, and homeostasis of other ECM proteins in the vocal fold lamina propria.[16,20] Together with HA, these proteoglycans likely contributed to the observed optimal viscoelastic properties of the acellular HUV construct and the recellularized scaffold as well. On the other hand, although Alcian blue staining demonstrated a widespread distribution of GAGs in the acellular HUV construct

(Fig. 3F), the potential detrimental effect of the cycles of osmotic stresses during the decellularization process on the various growth factors in the Wharton's jelly of the construct should be carefully addressed in future studies.

Clinically, the HUV has mostly been used as an allograft for cardiovascular reconstruction, such as peripheral vascular bypass surgery.[36,37] To our knowledge, Daniel *et al.*[23] performed the first study reporting the acellular HUV construct as a tissue engineering scaffold for developing small-diameter blood vessels for coronary and peripheral bypass. However, unlike the present study, the focus of that study was not primarily on the potential of the layer of Wharton's jelly on the acellular HUV construct for constructive matrix remodeling and extracellular tissue reconstruction, which is a distinct advantage of biological ECM scaffolds.[11,19]

One limitation of the current study was that the vocal fold fibroblasts were cultured statically in the acellular HUV construct. For functional vocal fold tissue engineering, in future studies, it will be necessary to apply physiologically relevant vibratory mechanical stimuli to the cultured cells, through bioreactors specially designed for delivering vibratory strain at phonatory frequencies, on the order of 100 Hz.[38,39] It has been well documented that mechanical signaling significantly influences the regulation of matrix protein–related messenger RNA expressions and protein expressions, and is critical to the development of functional tissue constructs with optimal biomechanical properties.[40] Another potential limitation of the current approach was that, ironically, endolaryngeal and phonomicrosurgical procedures that are designed to resect scar tissues, repair mucosal defects, and restore the mucosal wave could induce or aggravate vocal fold scarring, because the vocal fold layered structure is highly susceptible to scar tissue formation.[2,3] Current surgical approaches for vocal fold implantation have to be refined, and novel approaches addressing this dilemma have to be developed so that tissue engineering scaffolds can be delivered into the vocal fold lamina propria effectively.

Conclusions

This study reported the engineering of a decellularized ECM scaffold derived from the HUV with Wharton's jelly on its abluminal surface, with studies of its *in vitro* biocompatibility and biomechanical properties to examine the potential of the tissue construct for vocal fold regeneration. An acellular HUV construct with an intact ECM structure was fabricated through an optimized novel decellularization protocol previously developed in our laboratory, whereby cellular materials were removed using cycles of osmotic shock and nucleic acid digestion.[16] Primary-culture human vocal fold fibroblasts were seeded onto the acellular construct and their attachment, proliferation, and infiltration were examined with light microscopy, SEM, and cell recovery. The relative densities of newly synthesized collagen in the recellularized scaffolds were quantified with digital image analysis, and their viscoelastic properties were measured using a linear, simple-shear rheometer at frequencies of phonation. Results showed that primary vocal fold fibroblasts readily attached on the acellular HUV constructs, proliferated, and infiltrated the constructs, with significant cellular migration up to approximately 600 μm deep into the constructs. This extent of cellular infiltration was significantly higher than those reported previously.[14,16] A significant increase in the relative densities of collagen was observed in the recellularized scaffolds, indicative of active protein synthesis by the fibroblasts. The elastic shear modulus and the dynamic viscosity of the fibroblast-repopulated scaffolds at phonatory frequencies (100–250 Hz) were in the same range as those of the human vocal fold cover. These data suggested that the acellular HUV construct could be used as an allograft for the surgical repair of vocal fold lamina propria pathologies and tissue deficiencies, such as vocal fold scarring. Nevertheless, these findings should be regarded as preliminary *in vitro* data, with the need for further studies examining the *in vivo* host response in the vocal fold induced by the acellular construct.[29] Future studies should also address any inflammatory reaction and potentially adverse immune reaction that could be triggered by nonautologous allogeneic scaffolds such as the acellular HUV construct.

Acknowledgments

This work was supported by the National Institute on Deafness and Other Communication Disorders, National Institutes of Health grant R01 DC006101.

Disclosure Statement

No competing financial interests exist for any of the authors.

References

1. Benninger, M.S., Alessi, D., Archer, S., Bastian, R., Ford, C., Koufman, J., Sataloff, R.T., Spiegel, J.R., Woo, P. Vocal fold scarring: current concepts and management. Otolaryngol Head Neck Surg **115,** 474, 1996.
2. Hirano, S. Current treatment of vocal fold scarring. Curr Opin Otolaryngol Head Neck Surg **13,** 143, 2005.
3. Zeitels, S.M., Blitzer, A., Hillman, R.E., Anderson, R.R. Foresight in laryngology and laryngeal surgery: a 2020 vision. Ann Otol Rhinol Laryngol **116 Suppl. 198,** 2, 2007.
4. Chan, R.W., Titze, I.R. Viscoelastic shear properties of human vocal fold mucosa: measurement methodology and empirical results. J Acoust Soc Am **106,** 2008, 1999.
5. Chan, R.W., Titze, I.R. Dependence of phonation threshold pressure on vocal tract acoustics and vocal fold tissue mechanics. J Acoust Soc Am **119,** 2351, 2006.
6. Duflo, S., Thibeault, S.L., Li, W., Shu, X.Z., Prestwich, G.D. Vocal fold tissue repair in vivo using a synthetic extracellular matrix. Tissue Eng **12,** 2171, 2006.
7. Hahn, M.S., Teply, B.A., Stevens, M.M., Zeitels, S.M., Langer, R. Collagen composite hydrogels for vocal fold lamina propria restoration. Biomaterials **27,** 1104, 2006.
8. Jia, X., Yeo, Y., Clifton, R.J., Jiao, T., Kohane, D.S., Kobler, J.B., Zeitels, S.M., Langer, R. Hyaluronic acid-based microgels and microgel networks for vocal fold regeneration. Biomacromolecules **7,** 3336, 2006.
9. Sahiner, N., Jha, A.K., Nguyen, D., Jia, X. Fabrication and characterization of cross-linkable hydrogel particles based on hyaluronic acid: potential application in vocal fold regeneration. J Biomater Sci Polym Ed **19,** 223, 2008.
10. Badylak, S.F. Xenogeneic extracellular matrix as a scaffold for tissue reconstruction. Transplant Immunol **12,** 367, 2004.

11. Badylak, S.F. The extracellular matrix as a biologic scaffold material. Biomaterials **28,** 3587, 2007.
12. Cartwright, L.M., Shou, Z., Yeger, H., Farhat, W.A. Porcine bladder acellular matrix porosity: impact of hyaluronic acid and lyophilization. J Biomed Mater Res A **77,** 180, 2006.
13. Hudson, T.W., Zawko, S., Deister, C., Lundy, S., Hu, C.Y., Lee, K., Schmidt, C.E. Optimized acellular nerve graft is immunologically tolerated and supports regeneration. Tissue Eng **10,** 1641, 2004.
14. McFetridge, P.S., Daniel, J.W., Bodamyali, T., Horrocks, M., Chaudhuri, J.B. Preparation of porcine carotid arteries for vascular tissue engineering applications. J Biomed Mater Res **70A,** 224, 2004.
15. Schmidt, C.E., Baier, J.M. Acellular vascular tissues: natural biomaterials for tissue repair and tissue engineering. Biomaterials **21,** 2215, 2000.
16. Xu, C.C., Chan, R.W., Tirunagari, N. A biodegradable, acellular xenogeneic scaffold for regeneration of the vocal fold lamina propria. Tissue Eng **13,** 551, 2007.
17. Xu, C.C., Chan, R.W. Pore architecture of a bovine acellular vocal fold scaffold. Tissue Eng Part A **14,** 1893, 2008.
18. Young, B., Lowe, J.S., Stevens, A., Heath, J.W. Wheater's Functional Histology: A Text and Colour Atlas, 5th Ed. Philadelphia, PA: Elsevier, 2006.
19. Lai, P.H., Chang, Y., Chen, S.C., Wang, C.C., Liang, H.C., Chang, W.C., Sung, H.W. Acellular biological tissues containing inherent glycosaminoglycans for loading basic fibroblast growth factor promote angiogenesis and tissue regeneration. Tissue Eng **12,** 2499, 2006.
20. Sobolewski, K., Malkowski, A., Bankowski, E., Jaworski, S. Wharton's jelly as a reservoir of peptide growth factors. Placenta **26,** 747, 2005.
21. Gray, S.D., Titze, I.R., Chan, R., Hammond, T.H. Vocal fold proteoglycans and their influence on biomechanics. Laryngoscope **109,** 845, 1999.
22. Gray, S.D., Titze, I.R., Alipour, F., Hammond, T.H. Biomechanical and histologic observations of vocal fold fibrous proteins. Ann Otol Rhinol Laryngol **109,** 77, 2000.
23. Daniel, J., Abe, K., McFetridge, P.S. Development of the human umbilical vein scaffold for cardiovascular tissue engineering applications. ASAIO J **51,** 252, 2005.
24. Chan, R.W., Rodriguez, M.L. A simple-shear rheometer for linear viscoelastic characterization of vocal fold tissues at phonatory frequencies. J Acoust Soc Am **124,** 1207, 2008.
25. Rodriguez, M.L. The decellularized human umbilical vein (HUV) as an allogeneic scaffold for vocal fold tissue engineering. M.S. Thesis, University of Texas Southwestern Medical Center, Dallas, TX, 2007.
26. Thibeault, S.L., Li, W., Gray, S.D., Chen, Z. Instability of extracellular matrix gene expression in primary cell culture of fibroblasts from human vocal fold lamina propria and tracheal scar. Ann Otol Rhinol Laryngol **111,** 8, 2002.
27. Carson, F.L. Histotechnology. A Self-instructional Text, 2nd Ed. Chicago, IL: American Society of Clinical Pathologists, 1997.
28. Chan, R.W., Fu, M., Young, L., Tirunagari, N. Relative contributions of collagen and elastin to elasticity of the vocal fold under tension. Ann Biomed Eng **35,** 1471, 2007.
29. Xu, C.C., Chan, R.W., Weinberger, D.G., Efune, G., Pawlowski, K.S. A bovine acellular scaffold for vocal fold reconstruction in a rat model. J Biomed Mater Res Part A 2009 Jan 22. [Epub ahead of print].
30. Chan, R.W., Tayama, N. Biomechanical effects of hydration in vocal fold tissues. Otolaryngol Head Neck Surg **126,** 528, 2002.
31. Gogiel, T., Bankowski, E., Jaworski, S. Proteoglycans of Wharton's jelly. Intl J Biochem Cell Biol **35,** 1461, 2003.
32. Nanaev, A.K., Kohnen, G., Milovanov, A.P., Domogatsky, S.P., Kaufmann, P. Stromal differentiation and architecture of the human umbilical cord. Placenta **18,** 53, 1997.
33. Sobolewski, K., Bankowski, E., Chyczewski, L., Jaworski, S. Collagen and glycosaminoglycans of Wharton's jelly. Biol Neonate **71,** 11, 1997.
34. Valiyaveettil, M., Achur, R.N., Muthusamy, A., Gowda, D.C. Characterization of chondroitin sulfate and dermatan sulfate proteoglycans of extracellular matrices of human umbilical cord blood vessels and Wharton's jelly. Glycoconjugate J **21,** 361, 2004.
35. Ward, P.D., Thibeault, S.L., Gray, S.D. Hyaluronic acid: its role in voice. J Voice **16,** 303, 2002.
36. Dardik, H., Wengerter, K., Qin, F., Pangilinan, A., Silvestri, F., Wolodiger, F., Kahn, M., Sussman, B., Ibrahim, I.M. Comparative decades of experience with glutaraldehyde-tanned human umbilical cord vein graft for lower limb revascularization: an analysis of 1275 cases. J Vasc Surg **35,** 64, 2002.
37. Neufang, A., Espinola-Klein, C., Dorweiler, B., Messow, C.M., Schmiedt, W., Vahl, C.F. Femoropopliteal prosthetic bypass with glutaraldehyde stabilized human umbilical vein (HUV). J Vasc Surg **46,** 280, 2007.
38. Titze, I.R., Hitchcock, R.W., Broadhead, K., Webb, K., Li, W., Gray, S.D., Tresco, P.A. Design and validation of a bioreactor for engineering vocal fold tissues under combined tensile and vibrational stresses. J Biomech **37,** 1521, 2004.
39. Wolchok, J.C., Brokopp, C., Underwood, C.J., Tresco, P.A. The effect of bioreactor induced vibrational stimulation on extracellular matrix production from human derived fibroblasts. Biomaterials **30,** 327, 2009.
40. Freed, L.E., Guilak, F., Guo, X.E., Gray, M.L., Tranquillo, R., Holmes, J.W., Radisic, M., Sefton, M.V., Kaplan, D., Vunjak-Novakovic, G. Advanced tools for tissue engineering: scaffolds, bioreactors, and signaling. Tissue Eng **12,** 3285, 2006.

Address correspondence to:
Roger W. Chan
Biomedical Engineering
University of Texas Southwestern Medical Center
5323 Harry Hines Blvd.
Dallas, TX 75390-9035

E-mail: roger.chan@utsouthwestern.edu

Received: January 29, 2009
Accepted: May 20, 2009
Online Publication Date: July 10, 2009